QUANTIFICATION OF THE CONTRIBUTION OF FILLER CHARACTERISTICS TO NATURAL RUBBER REINFORCEMENT USING PRINCIPAL COMPONENT ANALYSIS

CINDY S. BARRERA,[1] ALFRED B. O. SOBOYEJO,[2] KATRINA CORNISH,[1,3]*

[1]FOOD, AGRICULTURAL AND BIOLOGICAL ENGINEERING, OHIO AGRICULTURAL RESEARCH AND DEVELOPMENT CENTER, THE OHIO STATE UNIVERSITY, WOOSTER, OH

[2]DEPARTMENT OF FOOD, AGRICULTURAL AND BIOLOGICAL ENGINEERING, THE OHIO STATE UNIVERSITY, COLUMBUS, OH

[3]HORTICULTURE AND CROP SCIENCE, OHIO AGRICULTURAL RESEARCH AND DEVELOPMENT CENTER, THE OHIO STATE UNIVERSITY, WILLIAMS HALL, 1680 MADISON AVENUE, WOOSTER, OH 44691

RUBBER CHEMISTRY AND TECHNOLOGY, Vol. 00, No. 0, pp. 000–000 (0000)

ABSTRACT

Practical statistical models were developed to quantify individual contributions from characteristics of conventional and non-conventional fillers and predict resulting mechanical properties of both hevea and guayule natural rubber composites. Carbon black N330 and four different agro-industrial residues, namely, eggshells, carbon fly ash, processing tomato peels, and guayule bagasse, were used in this study. Filler characteristics were used as explanatory variables in multiple linear regression analyses. Principal component analysis was used to evaluate correlations among explanatory variables based on their correlation matrices and to transform them into a new set of independent variables, which were then used to generate reliable regression models. Surface area, dispersive component of surface energy, carbon black, and waste-derived filler loading were found to have almost equal importance in the prediction of composite properties. However, models developed for ultimate elongation poorly explained variability, indicating the dependence of this property on other variables. Agro-industrial residues could potentially serve as more sustainable fillers for polymer composites than conventional fillers. This new modeling approach for polymer composites allows the performance of a wide range of different waste-derived fillers to be predicted with minimum laboratory work, facilitating the optimization of compound recipes to address specific product requirements. [doi:10.5254/rct.82.83716]

INTRODUCTION

Over 50,000 different products used on a daily basis worldwide are made with natural rubber,[1] most of them containing fillers. Fillers are commonly used in the rubber industry either as diluents or for the improvement of processing parameters and enhancement of properties such as modulus, tear strength, abrasion resistance, and tensile and compressive strength.[2–4] The reinforcement of rubber by fillers has been extensively studied for decades.[4–7] However, most of the research has focused on carbon black and silica fillers.

Different theories have been formulated to explain the mechanisms of reinforcement of natural rubber by fillers,[4] most of them based on the evaluation of performance properties affected by modifying a single filler characteristic, particularly surface area, thought to be the most important morphological characteristic affecting filler reinforcing potential.[2,8,9] Surface area and filler loading (amount of filler in the composites) determine the available interfacial area between the filler and the polymer.[3]

Filler structure also contributes to the reinforcing capability of the fillers by restricting polymer chain motion.[3,10] Filler particles can aggregate into complex tri-dimensional objects due to bonding forces between the particles.[8] Random spatial arrangement of the primary particles generates different degrees of irregularity that define the structure of the filler.[3] Complex filler structure also can result from naturally occurring pores and surface roughness. However, unlike surface area, this

*Corresponding author. Ph: 330-263-3982; email: cornish.19@osu.edu

filler characteristic is difficult to measure quantitatively. Also, different structures may coexist in a sample of the same filler due to the random aggregation, filler type, and production method.[2]

In general, filler characteristics govern the final mechanical properties of composites by determining the interaction between polymer and filler and the filler–filler interactions.[3,10] Surface activity must also be an important filler characteristic influencing rubber reinforcement because surface activity determines the ability of the filler to interact with the polymer. Differences in surface activity have been related to chemical groups on the surface of the particles[3,11] but may also result from structural heterogeneities.[8] These differences result in variations of surface free energy, a parameter that describes the interaction potential of a given surface.[12,13] Wetting experiments such as contact angle have been used for the evaluation of surface free energy of solid particles. However, these methods have been designed for macroscopic flat surfaces, and the accuracy of the measurements is limited by the size of the particles, surface roughness, and chemical heterogeneity.[14,15] Inverse gas chromatography (IGC) has proven to be a useful technique to characterize the surface of small particles.[16–18]

A complete understanding of the relationships between filler characteristics and macroscale mechanical properties of polymer composites has not been achieved. Furthermore, only limited attempts have been made to quantitatively estimate the contribution of each individual filler characteristic to the final composite properties and generate practical models to predict mechanical properties of rubber composites from filler characteristics.[19–21] Generally determining the extent to which different fillers reinforce a specific type of rubber requires extensive lab work. Molecular-level simulations require detailed information about the forces acting between the atomic centers, which is often not available. Furthermore, simulations performed at the atomic level are usually confined to relatively short oligomers[22] and cannot be applied effectively to rubber composites.

A statistical modeling approach is proposed to quantify the contribution of filler characteristics on mechanical properties of rubber composites and to establish functional relationships between these variables. We have developed data-driven models that best represent the relationship between the characteristics of different low cost, waste-derived, alternative fillers and mechanical properties of natural rubber composites.

EXPERIMENTAL

MATERIALS

Four waste-derived materials, namely, eggshells (ES), carbon fly ash (CFA), processed tomato peels (TP), and guayule bagasse (GB) were used. These materials were generously donated as follows: ES by Michael Foods (Gaylord, MN, USA) and Troyer's Home Pantry (Apple Creek, OH, USA); CFA by Cargill Salt (Akron, OH, USA); TP by Hirzel Canning Co. & Farms (Toledo, OH, USA). GB was generated as a co-product of latex extraction at our facility from guayule shrubs donated by PanAridus (Casa Grande, AZ, USA). Waste-derived materials were separately ground and sieved as described[23] to obtain macro-sized (diameter (d) of 300–38 μm) and micro-sized (d of 38 μm–100 nm) particles. Carbon black N330 (mean particle size, 108 nm; SD, 31.42 nm), was purchased from HB Chemicals (Twinsburg, OH, USA).

Probes used for particles' surface characterization included non-polar n-alkanes of different carbon chain length (C_5–C_9) and the polar probes, ethyl acetate, and dichloromethane. All probes were chromatographic grade and were purchased from Sigma-Aldrich (St. Louis, MO, USA). Physical constants of the probes were taken from the literature (Table I).[16] High purity methane purchased from Praxair Technology, Inc. (Akron, OH, USA), was used as a non-interacting probe.

TABLE I
PHYSICAL CONSTANTS OF THE PROBES

Probe	Cross-sectional area (a), 10^{-19} m^2	Surface tension (γ_1^D), J/m^2	Electron acceptor parameter (γ_I^+), J/m^2	Electron donor parameter (γ_I^-), J/m^2
Pentane	4.92	0.0155	—	—
Hexane	5.15	0.0179	—	—
Heptane	5.73	0.0203	—	—
Octane	6.30	0.0213	—	—
Nonane	6.90	0.0227	—	—
Dichloromethane	2.45	0.0245	0.0052	0
Ethyl acetate	3.30	0.0196	0	0.0192

FILLER CHARACTERIZATION

Inverse Gas Chromatography. — The fillers' surface energies were characterized by IGC, using a packed column gas chromatograph GC-2014 equipped with flame-ionization detector, Shimadzu Scientific Instruments (Columbia, MD, USA). Approximately 0.5–1.5 g of each filler were packed by mechanical vibration into stainless steel columns (50 cm long with inside diameter of 2.1 mm), and the two ends were plugged with silane-treated glass wool. The columns were shaped in a smooth "U" to fit the detector/injector geometry of the instrument. To minimize pressure drop across the GC column only macro-sized particles were used for the waste-derived materials. Carbon black was used as received.

The packed columns were preconditioned at 105 °C with 10 mL/min helium sweep for 12 h. After conditioning the columns, pulse injections were done with 0.04 μL for each of the probes. Retention times were determined at 50 and 100 °C, with the injector and detector kept at 180 and 200 °C, respectively. Helium was used as carrier gas. The flow rate was 20 mL/min for ES, TP, and GB; 40 mL/min for CB; and 60 mL/min for CFA. The retention times were determined from the median values of the elution peaks. Three columns were prepared for each material.

IGC Theoretical Background and Calculations. — The ability of a surface to interact with another surface depends on their individual surface energies. Surface free energy (γ_S) is the result of dispersive, γ_S^D, and specific components, γ_S^{SP}:[24]

$$\gamma_S = \gamma_S^D + \gamma_S^{SP} \tag{1}$$

IGC uses the relationship between the retention volume of the probes in contact with the filler surface and the thermodynamic parameters to determine these surface properties. This relation is given by the Gibbs free energy change equation:[17]

$$\Delta G_{ad}^0 = \Delta G_{ed}^0 = RT\ln V_N + C \tag{2}$$

where ΔG_{ad}^0 and ΔG_{ed}^0 are the standard molar Gibbs free energy changes of adsorption and desorption, R is the gas constant (8.314 J/K * mol), T is absolute temperature, and C is the integration constant. V_N is the net retention volume of the probe, and is calculated as

$$V_N = JF_c(t_R - t_0) \tag{3}$$

where J is the James–Martin compressibility correction factor, F_c is the temperature corrected flow rate of the carrier gas, t_R is the retention time of the probe, and t_0 is the

dead time determined from the retention time of a non-interacting probe (methane). V_N can be divided by the mass and surface area of the particles to obtain a specific retention volume.[25]

Non-polar probes such as *n*-alkanes only will interact through London dispersive forces,[26] even when they come into contact with polar surfaces. This characteristic has been used to quantify the dispersive component of the surface of solids. The dispersive component can be calculated using the method proposed by Schultz and Lavielle:[17,24,25]

$$RT\ln V_N = 2Na\sqrt{\gamma_S^D \times \gamma_L^D} + C \tag{4}$$

where a is the cross-sectional area of the probe, N is Avogadro's number (6.023×10^{23}/mol), and γ_S^D and γ_L^D are the dispersive components of surface free energy of the solid and the probe, respectively. For a series of *n*-alkanes, γ_S^D is calculated from the slope of $RT \ln V_N$ versus $a\sqrt{\gamma_L^D}$.

Unlike non-polar probes, which only interact with the solid surface through dispersive forces, polar probes can interact with a solid surface through both dispersive and specific interactions. Therefore, the standard molar Gibbs free energy change of adsorption for the interaction of the polar probe and the surface under investigation[17,27] is

$$\Delta G_{\text{ad}}^0 = \Delta G_{\text{ad}}^D + \Delta G_{\text{ad}}^{\text{SP}} \tag{5}$$

where ΔG_{ad}^D and $\Delta G_{\text{ad}}^{\text{SP}}$ are the dispersive and specific free energies of adsorption. $\Delta G_{\text{ad}}^{\text{SP}}$ has been described in terms of the tendency of a surface to behave as either an electron acceptor or an electron donor. These surface characteristics can be calculated using the Good–van Oss equation:[27]

$$\Delta G^{\text{SP}} = 2Na\left(\sqrt{\gamma_I^+ \times \gamma_S^-} + \sqrt{\gamma_I^- \times \gamma_S^+}\right) \tag{6}$$

where γ_S^+ and γ_S^- are the electron acceptor and electron donor parameters of the solid surface, and γ_I^+ and γ_I^- are the electron acceptor and electron donor parameters of the probe. Monopolar acidic and basic probes such as dichloromethane and ethyl acetate are used to measure γ_S^+ and γ_S^-, which allows the calculation of the specific component of the surface of solid (γ_S^{SP}):[16,27]

$$\gamma_S^{\text{SP}} = 2\sqrt{\gamma_S^+ \times \gamma_S^-} \tag{7}$$

Evaluation of surface energy through IGC is based on the assumption that adsorption and desorption equilibrium conditions between adsorbent and adsorbate are achieved. This condition is satisfied by injecting very low concentrations of probes, which results in linear adsorption isotherms and symmetrical chromatographic peaks. This chromatographic condition is known as infinite dilution. Owing to the limited amount of probe, interaction occurs only with the high-energy sites on the surface, and no probe to probe interactions are expected, enabling an accurate and reproducible calculation of the retention volume.[17,28,29]

Surface area and pore size distribution. — Surface area and pore size distribution of the waste-derived fillers were determined from nitrogen adsorption–desorption isotherms at 77 K. The samples were analyzed using a Tristar II 3020 analyzer, Micromeritics Instrument Corporation (Norcross, GA, USA). The particles were degassed at room temperature for 12 h prior to analysis. Surface area was calculated using the Brunaure–Emmett–Teller method,[30] while pore size distribution was calculated using the Barrett–Joyner–Halenda method.[31] Carbon black surface area was obtained from the specification provided by the supplier.

TABLE II
NOTATION OF DIFFERENT EXPERIMENTAL DATA USED FOR STATISTICAL ANALYSES

Variable notation	Experimental data for model
Y_1	300% modulus, MPa
Y_2	Ultimate elongation, %
Y_3	Tensile strength, MPa
X_1	Total filler surface area, m^2
X_2	Dispersive component of filler surface free energy, mJ/m^2
X_3	Specific component of filler surface free energy, mJ/m^2
X_4	Carbon black loading, phr[a]
X_5	Waste-derived filler loading, phr[a]

[a] phr: parts per hundred rubber

STATISTICAL ANALYSIS

Data. — Mechanical properties for the guayule and hevea rubber composites used in this study were determined in previous work.[23,32] These data include mechanical properties of vulcanized composites manufactured by partially and fully replacing carbon black with different waste-derived fillers, composites made solely with carbon black, and unfilled rubber compounds.

Data normality and constant variance assumptions were tested using the Shapiro–Wilk normality test[33] and visualized by histograms. The variables were categorized into response variables (Y_i) which represent the different mechanical properties of the composites, and explanatory variables (X_i), which represent filler characteristics (Table II). The data were standardized by subtracting the mean and dividing by the standard deviation before statistical analysis.

Principal Component Analysis. — Principal component analyses (PCA) were used to evaluate correlations among the variables based on their correlation matrices and to transform correlated explanatory variables. In order to produce reliable probabilistic models, all explanatory variables sould be completely independent. However, this is rarely the case in biological and engineering systems. PCA is used to transform all the correlated explanatory variables into uncorrelated sets of new variables that account for the majority of the original variance (principal component scores).[34–37] This is done by using a procedure that applies a matrix method as an essential mathematical tool. The new standardized uncorrelated explanatory variables are given by Eq. 8.

$$[PC]=[X][T] \tag{8}$$

where [**PC**] corresponds to the value of the principal components and [**T**] is the matrix of principal component loadings that multiplies the standardized original explanatory variables [**X**].[34,38] PCA was perfomed using the Stats package implemented in R.[39] Principal component (PC) scores were used as independent variables in multiple linear regression analysis to predict mechanical properties of the composites.

Multiple Linear Regression. — Multiple linear regression (MLR) analysis was used to develop models using JMP 11 Statistical Analysis Software (SAS Institute Inc., Cary, NC, USA). Two different approaches were applied for model development. In the first approach, filler characristics were used as explanatory variables (Table II) to predict the composites' mechanical properties, whereas in the second approach, PC scores obtained from PCA of filler characteristics were used to predict tensile properties.

TABLE III
FILLERS' SURFACE AREA AND PORE VOLUME

Filler	Surface area, m^2/g	Pore volume, mm^3/g^b
Carbon black N330	80.2[a]	—
Carbon fly ash micro	10.440	21.391
Carbon fly ash macro	4.241	5.961
Eggshells micro	1.075	5.368
Eggshells macro	0.224	0.676
Guayule bagasse micro	0.482	0.730
Guayule bagasse macro	0.716	1.108
Tomato peels micro	0.852	1.409
Tomato peels macro	0.016	—

[a] Cetyl trimethyl ammonium bromide (CTAB) surface area.
[b] Barrett–Joyner–Halenda adsorption cumulative pore volume.

The standard format for the regression models is represented by Eq. 9.

$$Y = f(X_1, X_2 \ldots X_k) = a + \sum_{i=1}^{k} b_i X_i \tag{9}$$

where Y is the response variable, $X_1, X_2, \ldots, X_k$ are the predictor variables, and a, b_i for $i=1, 2, \ldots, k$ are the model constants.[38] Non-significant terms were excluded from the models. Model adequacy was evaluated based on residuals analysis. Coefficient of determinations (R^2) and adjusted R^2, were reported.

RESULTS AND DISCUSSION

FILLER CHARACTERIZATION

Carbon black had the highest specific surface area among all the fillers (Table III). This is due to its small particle size (108 ± 31 nm). In general, specific surface area of all the waste-derived fillers increased with decreasing particle size, except in the case of GB. For this filler, the micro-sized particles had a lower surface area than the macro-sized particles, possibly due to a decrease in aspect ratio. Grinding of the GB not only reduced the diameter of the fiber but also the length. CFA had the largest specific surface area, both for macro- and micro-sized particles, due to its small particle size and high porosity. CFA had the smallest mean particle size for both the macro-sized particles (89.32 ± 61.94 μm) and micro-sized particles (12.12 ± 4.93 μm),[32] and the highest pore volume (Table III).

Variations in filler surface energy were observed among the different materials (Table IV), due to differences in energy sites where the interaction between the filler and the adsorbate occurs. These sites correspond to chemical and structural heterogeneities in the surface of the material.[40] Carbon black had the highest dispersive component (γ_S^D) among the fillers used. Also, this was the only filler with a higher dispersive than specific component (γ_S^{SP}) of surface energy. All the waste-derived fillers had a higher specific than dispersive component. A low specific component indicates that the contribution of specific interactions in the adsorption of the filler is small and the surface of the material is mostly only capable of interaction through London type interactions.[16,41] Given the non-polar character of natural rubber, dispersive forces play the main role in the interaction with the

TABLE IV
FILLERS' SURFACE PROPERTIES

	50 °C			100 °C		
Filler	γ_S^D,[a] mJ/m^2	γ_S^{SP},[b] mJ/m^2	γ_S,[c] mJ/m^2	γ_S^D, mJ/m^2	γ_S^{SP}, mJ/m^2	γ_S, mJ/m^2
Carbon black	162.273	80.357	242.630	128.564	63.926	192.490
Carbon fly ash	119.594	—		108.474	126.787	235.261
Eggshells	21.035	53.318	74.353	11.454	21.281	32.735
Guayule bagasse	42.430	120.832	163.262	26.151	78.545	104.696
Tomato peels	46.136	216.174	262.310	29.276	151.576	180.852

[a] γ_S^D, Dispersive component of surface energy.
[b] γ_S^{SP}, Specific components of surface energy.
[c] γ_S, Total surface free energy.

filler. Therefore, composites containing fillers with high specific components have been associated with weak polymer–filler interactions and strong filler–filler interactions.[8]

Carbon black surface energy can be explained by its particular chemical composition and structure. Carbon blacks are mainly elemental carbon in the form of graphitic crystallites with some amorphous regions. However, they also contain small quantities of other components, namely, hydrogen, oxygen, and sulfur.[8,42] CFA had both high dispersive and specific components and overall the highest total surface energy (γ_S). CFA has a varying amount of unburned carbon (20–1%), but it is mainly amorphous alumino-silicate (over 50%) and also possesses large quantities of iron, calcium, potassium, magnesium, sodium, and sulfur compounds.[43,44] These polar groups on the surface of the CFA are able to exchange both dispersive and specific interaction.

GB and TP both had high specific components and relatively low dispersive components (Table IV). This can be attributed primarily to the presence of a large number of polar groups, such as hydroxyl and carboxyl groups. However, both GB and TP are a complex assembly of biopolymers in which structural heterogeneities also contribute to their surface energy. TP consists of a thin cuticle layer, attached to the epidermal cell wall by a pectinaceous layer.[45,46] The cell wall is composed of cellulose and hemicellulose, structural proteins, and other non-polysaccharide components such as phenolics.[46] The cuticle layer is composed mostly of cutin, which is a polyester rich in hydroxyl and epoxy fatty acids,[45,47] overlaid with wax. GB is a ligno-cellulosic residue and also contains approximately 10% terpene resin.[48,49]

ES had the lowest dispersive and specific components among all the fillers, due to its crystalline structure. ES is 95% calcium carbonate crystals.[50,51] Surface energy of the solid is not only dependent on the chemical composition, but also the accessibility to high-energy sites, which is determined by arrangement and orientation of chemical groups in the surface.[18] Materials containing an amorphous fraction present a higher surface energy than well crystallized materials.[52] Other components in ES include magnesium carbonate, calcium phosphate, and organic matter.[51,53]

Both dispersive and specific components decreased with increasing temperature for all the fillers tested. This is likely due to desorption of surface impurities that contributes to the surface energy at lower temperatures. Very broad peaks were obtained when ethyl acetate was injected as a polar probe in CFA columns at 50 °C, which made it impossible to accurately determine the peak maximum. Therefore, surface properties at 100 °C were used for the statistical analysis.

STATISTICAL ANALYSIS

Analysis of the Data. — Tensile strength and 300% modulus were highly positively correlated with total filler surface area, dispersive component and carbon black loading, and negatively correlated with waste-derived filler loading, in both guayule and hevea composites (Figure 1; Table V). PCA biplots show graphically the correlation among variables (Figure 1). Each vector represents a variable, and the correlation between any pair of variables is determined by the angle between them. Vectors orthogonal to each other (90° angle) are independent from each other. If the angle between two vectors is close to 0° these variables are highly positively correlated, but if the angle is close to 180° the pair of variables are highly negatively correlated.

The results obtained are in agreement with existing literature about the reinforcement of natural rubber by fillers. The enhancement of these properties by filler is generally attributed to strong polymer–filler interactions.[4] Non-polar elastomers like natural rubber will mainly interact through dispersive forces, and carbon black has a higher dispersive component of surface energy than the waste-derived fillers studied (Table IV). Filler surface area determines the available contact area for these interactions to occur. Negative correlations of tensile strength and 300% modulus and waste-derived filler loading are due to particular characteristics of the filler studies and reflect the general trend among the different fillers.

Although ultimate elongation was correlated to the same filler characteristics as tensile strength and 300% modulus, the magnitude of the correlation coefficients was generally lower (Table V). Overall, filler characteristics had an opposite effect on ultimate elongation than 300% modulus and tensile strength.

Two-way interaction plots also were made to check for interactive effects among the different response variables (Figures 2 and 3). Owing to the high correlation between waste-derived filler loading and carbon black loading, only waste-derived filler loading was used in the analyses. Fillers' dispersive and specific surface energy components were combined into filler type, and particle size range was used instead of the surface area. In the two-way interaction plot, interactive effects between two explanatory variables on the response variables are indicated if the plotted lines are not parallel to each other.

Interactive effects were observed particularly between waste-derived filler loading and type of filler for both hevea and guayule composites. These interactions indicate that the effect of one predictor variable on the response variable is different at different values of the other predictor variable. Interactive effects between filler characteristics are understandable in rubber composites due to the complexity of these systems. The contribution of the filler network to final composite properties is an example of these interactive effects. A specific volume of particles, known as the percolation threshold, is required in order to form this network. The percolation threshold depends on the filler used. Different fillers will have different percolation thresholds due to differences in aspect ratio.[32,54] This means that the effect of the filler type will be different depending on whether the loading is above or below the percolation threshold. Hence, interactive effects between filler characteristics were included in the regression models.

Multiple Regression Analysis. — Regression models were developed for each of the response variables both for hevea and guayule composites based on the explanatory variables and their interactions (Table VI). These models excluded variables that were found not significant ($p > 0.05$). Coefficients of determination indicate the proportion of the variability explained by the model.

The models proposed account for over 90% of the variability observed in the 300% modulus response, for both guayule and hevea composites (Eqs. 10 and 13). In contrast, the models fitted for ultimate elongation accounted for 74% of the variability in hevea composites and only 35% in guayule composites (Eqs. 11 and 14). Approximately 83% and 82% of the variability in tensile

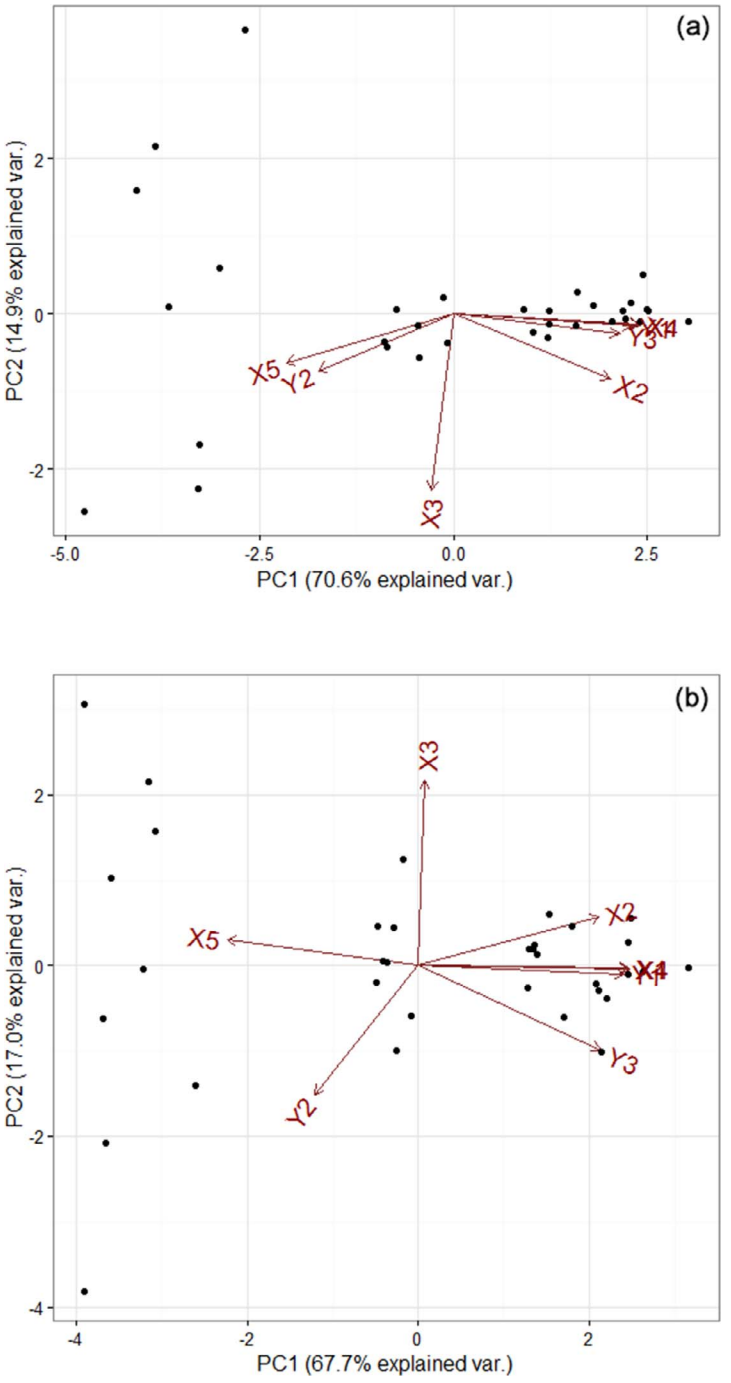

FIG. 1. — Biplot generated by principal component analysis. (a) Hevea composites, (b) Guayule composites. PC1 is the first principal component and PC2 is the second principal component. *Y*1, 300% modulus; *Y*2, ultimate elongation; *Y*3, tensile strength; *X*1, total filler surface area; *X*2, dispersive component of surface energy; *X*3, specific component of surface energy; *X*4, carbon black loading; *X*5, waste-derived filler loading.

TABLE V
CORRELATION MATRIX

	Total filler surface area	γ_S^{D}[a]	γ_S^{SP}[b]	Carbon black loading	Waste-derived filler loading	300% modulus	Ultimate elongation	Tensile strength
Hevea composites								
Total filler surface area	1.000	0.837	−0.068	0.997	−0.856	0.937	−0.667	0.884
γ_S^{D}		1.000	0.170	0.830	−0.619	0.721	−0.503	0.737
γ_S^{SP}			1.000	−0.069	0.290	−0.041	0.215	−0.108
Carbon black loading				1.000	−0.867	0.929	−0.663	0.873
Waste-derived filler loading					1.000	−0.784	0.719	−0.700
300% modulus						1.000	−0.654	0.905
Ultimate elongation							1.000	−0.366
Tensile strength								1.000
Guayule composites								
Total filler surface area	1.000	0.839	0.036	0.997	−0.867	0.955	−0.453	0.866
γ_S^{D}		1.000	0.284	0.832	−0.646	0.745	−0.401	0.698
γ_S^{SP}			1.000	0.033	0.159	−0.005	−0.256	−0.187
Carbon black loading				1.000	−0.876	0.960	−0.456	0.868
Waste-derived filler loading					1.000	−0.849	0.486	−0.732
300% modulus						1.000	−0.476	0.858
Ultimate elongation							1.000	−0.011
Tensile strength								1.000

[a] γ_S^{D}, Dispersive component of surface energy.
[b] γ_S^{SP}, Specific components of surface energy.

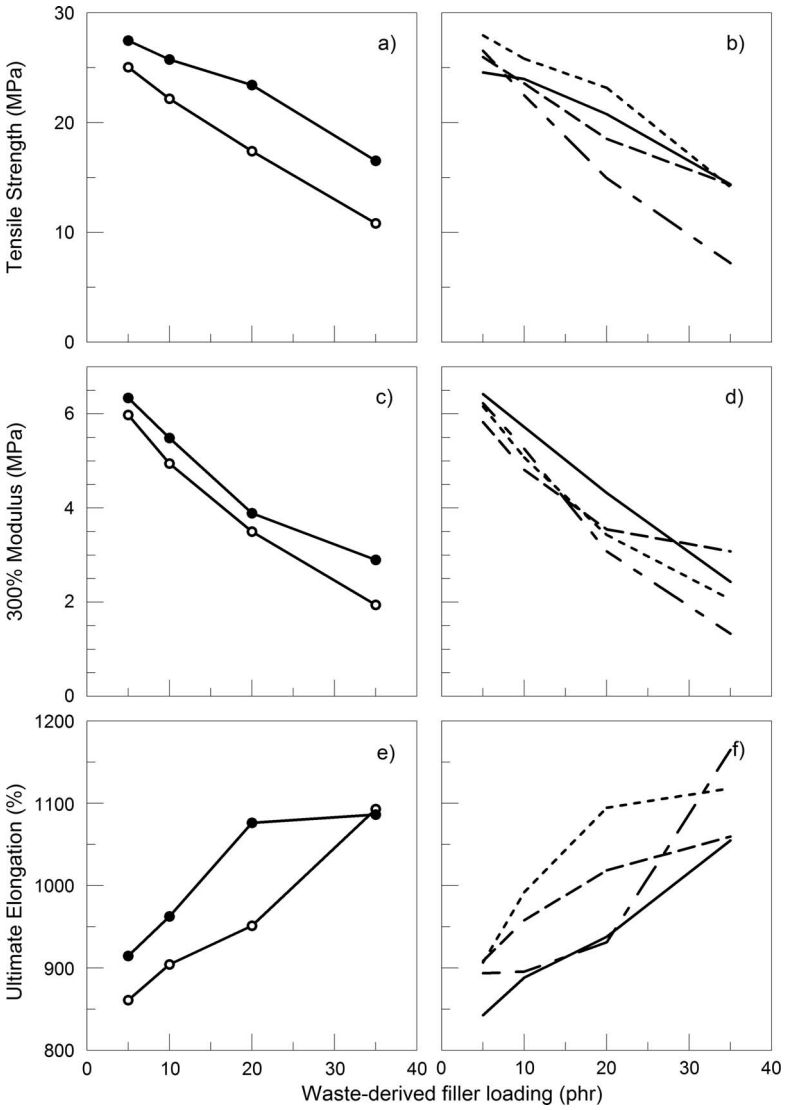

FIG. 2. — Interaction of waste-derived filler loading with particle size (a, c, e) and waste-derived filler type (b, d, f) on mechanical properties of hevea composites. Particle size: macro —o—, micro —●—; waste-derived filler type: carbon fly ash ——, eggshells ·····, guayule bagasse – – –, tomato peels – · –.

strength for hevea and guayule composites, respectively, was explained by the proposed models (Eqs. 12 and 15). The low portion of variability explained by the models proposed for ultimate elongation, particularly for guayule composites, indicates that other effects not considered have a significant influence on this particular property.

Differences in variable combinations and the magnitude of model parameters between models generated for hevea and guayule composites for the same response variable also were found. These differences are mostly due to chemical and structural differences between these two natural rubbers and the way they interact with the fillers. However, they are also a consequence of multicollinearity within the data. Filler characteristics used as explanatory variables were strongly correlated among

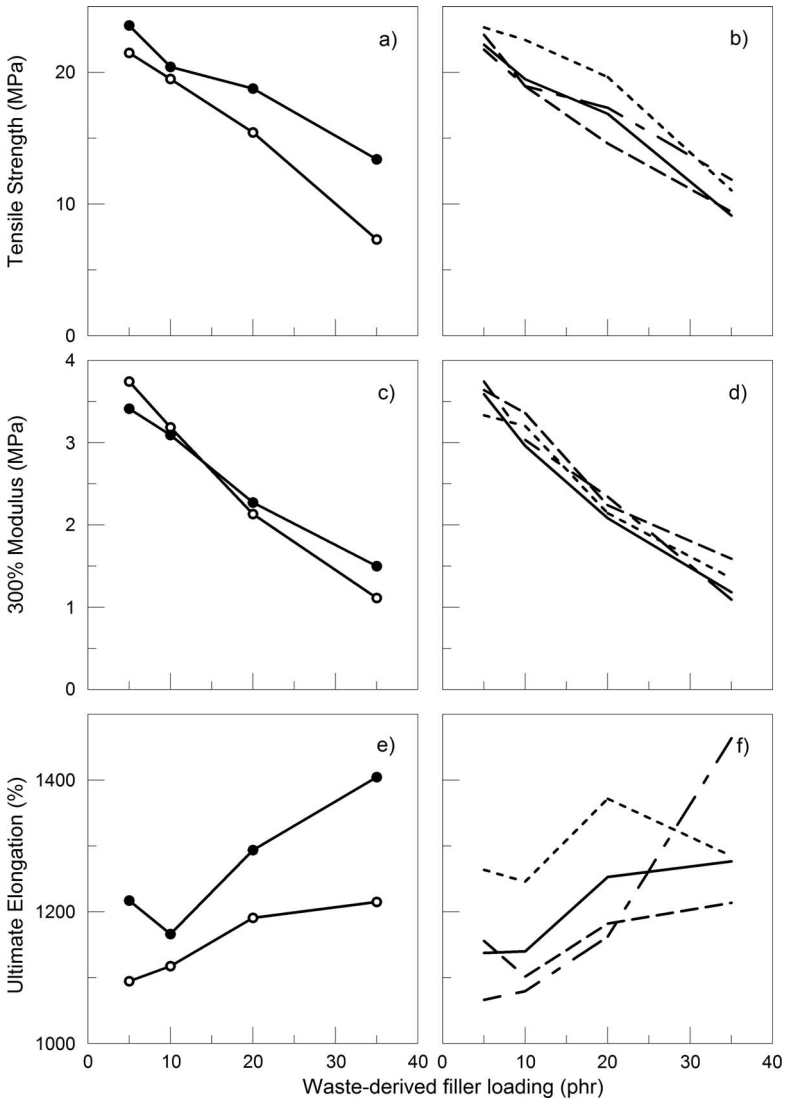

FIG. 3. — Interaction of waste-derived filler loading with particle size (a, c, e) and waste-derived filler type (b, d, f) on mechanical properties of guayule composites. Particle size: macro —○—, micro —●—; waste-derived filler type: carbon fly ash ——, eggshells-----, guayule bagasse – – –, tomato peels – · –.

each other (Table V). The presence of such strong multicollinearity makes the models obtained with the original explanatory variables unable to determine the real effect of the filler characteristics on the response variables.

Regression models were developed using PC scores that resulted from the transformation of explanatory variables using PCA (Table VII). Nearly 90% of the variability in the 300% modulus response was explained by the regression model (Eqs. 16 and 19) for both hevea and guayule composites (Figure 4a and 4b), whereas the models generated for tensile strength (Eqs. 18 and 21) accounted for approximately 80% of the variability observed for both rubbers (Figure 4e and 4f). Common variables in all of these models are PC_1 and PC_4. These two components' main contributions are attributed to total filler surface area and carbon black and waste-derived filler

TABLE VI
REGRESSION MODELS USING THE STANDARDIZED ORIGINAL INDEPENDENT VARIABLES

Regression Equation	R^2	Adjusted R^2	Equation number
Hevea composites			
$Y_1 = -0.541 - 4.759X_1 + 3.924X_5 + 2.765X_1X_4 - 2.536X_4X_5$	0.922	0.910	10
$Y_2 = 0.714 - 16.092X_3 - 0.692X_4 + 0.536X_5 - 10.722X_3X_4$	0.743	0.705	11
$Y_3 = 0.404 - 9.177X_3 + 0.589X_4 - 6.065X_3X_4$	0.835	0.817	12
Guayule composites			
$Y_1 = (-2.94e - 16) - 0.175X_2 + 1.106X_4$	0.931	0.927	13
$Y_2 = (5.14e - 16) - 0.342X_3 + 0.540X_5$	0.350	0.308	14
$Y_3 = 0.082 + 0.540X_3 - 0.817X_5 - 0.533X_3X_5$	0.820	0.802	15

loading (Table VIII). For both 300% modulus and tensile strength, PC_1 had a positive effect on the response, while PC_4 had a negative impact as indicated by the sign of the coefficients (Table VII). This means that a total increase in total filler surface area and carbon black loading will generate an increase in the responses proportional to their contribution in the model. On the other hand, an increase in waste-derived filler loading would adversely affect these two responses for both guayule and hevea.

PC_5 was found to have a significant effect for 300% modulus in hevea composites (Eq. 16) but not in guayule composites (Eq. 19). However, owing to the low percentage of the portion of the variance in the filler characteristics explained by PC_5 (<0.1%) (Table VIII), the removal of this effect from the model (Eq. 16) will only slightly reduce the R^2 to 0.880. PC_2 was included as a significant factor for the prediction of tensile strength for guayule composites (Eq. 21) but was not significant for the same response in hevea composites (Eq. 18) and so was not included here. Unlike the models fitted for modulus, the removal of PC_2 will have a greater impact on the prediction of tensile strength (R^2 decreased from 0.80 to 0.75) for guayule composites due to the larger portion of the variance in filler characteristics explained by PC_2 (>22%) (Table VIII).

PC_2 had a negative effect on the tensile strength of guayule rubber composites. This component is heavily influenced by specific components of surface energy, which indicates that this filler characteristic is important in predicting the tensile strength of guayule composites but not of hevea composites. This is due to the impact that this filler characteristic has on the vulcanization of the

TABLE VII
REGRESSION MODELS USING PRINCIPAL COMPONENT SCORES

Regression Equation	R^2	Adjusted R^2	Equation number
Hevea composites			
$Y_1 = (-5.09e - 7) + 0.481PC_1 - 0.810PC_4 - 2.475PC_5$	0.896	0.885	16
$Y_2 = (-4.573e - 7) - 0.3666PC_1$	0.471	0.454	17
$Y_3 = (-6.254e - 7) + 0.456PC_1 - 0.765PC_4$	0.792	0.778	18
Guayule composites			
$Y_1 = (-8.047e - 7) + 0.497PC_1 - 0.663PC_4$	0.914	0.909	19
$Y_2 = (2.258e - 7) + 0.256PC_1$	0.232	0.208	20
$Y_3 = (-8.447e - 7) + 0.446PC_1 - 0.210PC_2 - 0.662PC_4$	0.800	0.780	21

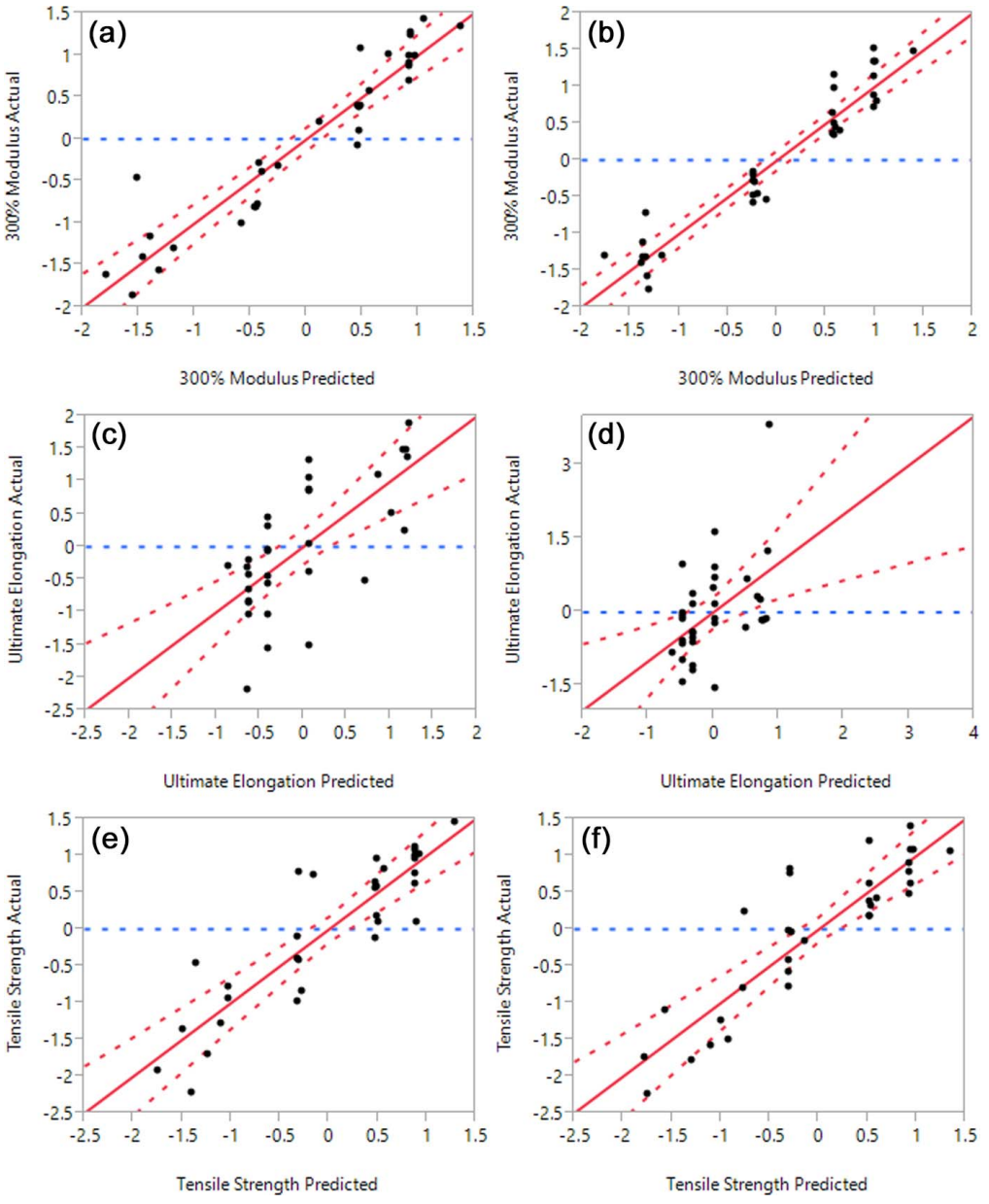

FIG. 4. — Standardized observed vs values predicted by regression models using principal component scores. (a) 300% modulus, (c) ultimate elongation, and (e) tensile strength of hevea composites; (b) 300% modulus, (d) ultimate elongation, and (f) tensile strength of guayule composites. The red solid line represents the regression line; the red dashed lines indicate the 95% confidence intervals; and the horizontal blue dashed line represents the mean response observation.

rubber. A high specific component results from a more chemically active surface. These highly active surfaces can interact with compounding ingredients, affecting the cure kinetics, and leading to differences in crosslink density that affect mechanical properties.[11] Given that the same curing system was used for all composites, this variable is more important in guayule than hevea because of

TABLE VIII
PRINCIPAL COMPONENT LOADINGS

	PC1[a]	PC2	PC3	PC4	PC5
Hevea composites					
Total filler surface area	**0.526**	0.026	0.037	−0.482	**−0.699**
γ_S^{D}[b]	0.462	0.309	**−0.701**	0.446	0.015
γ_S^{SP}[c]	−0.053	**0.917**	0.394	0.038	−0.011
Carbon black loading	**0.526**	0.022	0.083	−0.454	**0.714**
Waste-derived filler loading	−0.479	0.251	**−0.587**	**−0.601**	0.032
Eigen value	3.520	1.133	0.243	0.100	0.003
Standard deviation	1.876	1.065	0.493	0.317	0.051
Proportion of variance	0.704	0.227	0.049	0.020	0.001
Cumulative proportion	0.704	0.931	0.979	0.999	1.00000
Guayule composites					
Total filler surface area	**0.524**	−0.032	0.007	−0.482	**−0.701**
γ_S^{D}	0.470	0.272	**−0.702**	0.461	0.016
γ_S^{SP}	0.037	**0.925**	0.379	−0.006	−0.007
Carbon black loading	**0.525**	−0.039	0.049	−0.463	**0.712**
Waste-derived filler loading	−0.477	0.262	**−0.601**	**−0.585**	0.027
Eigen value	3.541	1.126	0.227	0.103	0.002
Standard deviation	1.882	1.061	0.477	0.321	0.050
Proportion of variance	0.708	0.225	0.045	0.021	0.001
Cumulative proportion	0.708	0.933	0.979	0.999	1.00000

[a] PC, principal component.
[b] γ_S^{D}, Dispersive component of surface energy.
[c] γ_S^{SP}, Specific components of surface energy.

differences in vulcanization behavior. Guayule rubber has lower curing rates due to different non-rubber components than hevea.[55,56]

Contrary to 300% modulus and tensile strength, the variability explained by the models generated for ultimate elongation was lower than 50% (Figure 4c and 4d) (Eqs. 17 and 20). This means that other, unmeasured, variables contribute to the observed ultimate elongation. Filler structure is an example of an unaccounted variable. Filler structure has been associated with changes in ultimate elongation in carbon black composites.[8,42] Fillers with highly irregular surfaces due to branched aggregates and/or porosity restrict chain motion under applied strain and contribute to physical crosslinking of rubber. Chemistry related variables such as the pH of the fillers also may affect crosslink density and hence properties such as ultimate elongation. Alkaline fillers like ES can cause faster curing rates, which can lead to higher crosslink density.[11,32] Finally the presence of terpene resins, such as those in GB, can also have an effect on resulting composite properties. These resins can act as plasticizers, which would increase ductility of the materials.[23]

It is important to notice that PC_1 is a comon variable in all the models (Table VII). This is because this component alone accounts for over 70% of the total variation in the original explanatory variables (Table VIII). PC_1 is also slightly influenced by the dispersive component of surface energy and the waste-derived filler loading.

Despite the lower R^2 for the models developed with the transformed explanatory variables (Table VII), these models are more reliable than the models developed using the original explanatory variables (Table VI), which were highly correlated. Multicollinearity does not reduce

the overall predicting power of the model, but it drastically affects the calculation of regression equation. In regression models containing correlated explanatory variables, the variances of the regression coefficients can become very large.[34] This compromises the model's ability to accurately identify real contributions of the filler characteristic on a given response variable.

CONCLUSIONS

The statistical modeling approach employed proved to be an efficient tool for the estimation of individual contributions of different filler characteristics on the properties of both guayule and hevea natural rubber composites. This is important, considering the complexity of these systems and the wide range of possible alternative fillers that remain unexplored. Furthermore, this modeling approach can be used to predict properties in different polymer composites based on specific polymer and filler characteristics, compounding formulations, and processing conditions. Filler surface area and loading were found to be important variables contributing to composite properties, particularly for 300% modulus and tensile strength. However, the new models demonstrate that a single variable cannot predict all properties of rubber composites due to their complexity. Therefore, a combination of two or more filler characteristics is required to provide a good fit. The identification of the contribution of each filler characteristic to particular properties makes it easier to target a particular material or combination of materials as potential fillers for a given composite application based on the desired performance properties. This modeling method can facilitate the screening of a large number potential non-conventional fillers and hybrid filler composites and the optimization of properties.

ACKNOWLEDGEMENTS

We thank Ohio Third Frontier, Ohio Research Scholars Program in Technology-Enabling and Emergent Materials (TECH 09-026), Institute for Materials Research Facility Grant, The Ohio State University, and USDA National Institute of Food and Agriculture (Hatch project 230837) for providing financial support for this project. We also thank the Fulbright Foundation for sponsoring Cindy Barrera during her Ph.D. Program.

REFERENCES

[1]P. M. Priyadarshan, in *Biology of Hevea Rubber*, CABI, Wallingford, UK, 2011, pp. 1–6.

[2]J. B. Donnet and E. Custodero, in *The Science and Technology of Rubber*, Elsevier, 4th ed., 2013.

[3]J. Fröhlich, W. Niedermeier, and H. D. Luginsland, *Compos. Part A Appl. Sci. Manuf.* **36**, 449 (2005).

[4]A. Bin Samsuri, "Theory and Mechanisms of Filler Reinforcement in Natural Rubber," in *Natural Rubber Materials: Volume 2: Composites and Nanocomposites*, H. M. Sabu Thomas, Chin Han Chan, Laly Pothen, Jithin Joy, Eds., The Royal Society of Chemistry, London, 2013, vol. 2, pp. 73–111.

[5]J. W. Watson, RUBBER CHEM. TECHNOL. **30**, 987 (1956).

[6]R. S. Bradley, *J. Colloid. Sci.* **11**, 237 (1956).

[7]A. R. Payne, *J. Appl. Polym. Sci*. **6**, 368 (1962).

[8]J. Leblanc, *Prog. Polym. Sci*. **27**, 627 (2002).

[9]I. Khan and A. H. Bhat, "Micro and Nano Calcium Carbonate Filled Natural Rubber Composites and Nanocomposites" in *Natural Rubber Materials. Composites and Nanocomposites*, H. M. Sabu Thomas, Chin Han Chan, Laly Pothen, Jithin Joy, Eds., The Royal Society of Chemistry, London, 2014, pp. 467–487.

[10]D. J. Kohls and G. Beaucage, *Curr. Opin. Solid State Mater. Sci*. **6**, 183 (2002).

[11]J. T. Byers, in *Basic Elastomer Technology*, K. C. Baranwal and H. L. Stephens, Eds., American Chemical Society, Rubber Division, Akron, OH, 2001, pp. 82–111.

[12]N. Cordeiro, C. Gouveia, and M. J. John, *Ind. Crops Prod.* **33**, 108 (2011).

[13]M. Nardin, H. Balard, and E. Papirer, *Carbon N. Y.* **28**, 43 (1990).

[14]B. B. Hole, D. S. Keller, W. M. Burry, and J. A. Schwarz, *J. Chromatogr. B Anal. Technol. Biomed. Life Sci.* **879**, 1847 (2011).

[15]B. Riedl and L. M. Matuana, "Inverse Gas Chromatography of Fibers and Polymers," in *Encyclopedia of Surface and Colloid Science*, 2nd ed., Taylor & Francis, New York, 2006.

[16]B. Strzemiecka, A. Voelkel, J. Donate-Robles, and J. M. Martín-Martínez, *Appl. Surf. Sci.* **316**, 315 (2014).

[17]S. Mohammadi-Jam and K. E. Waters, *Adv. Colloid Interface Sci.* **212**, 21 (2014).

[18]N. Cordeiro, C. Gouveia, A. G. O. Moraes, and S. C. Amico, *Carbohydr. Polym.* **84**, 110 (2011).

[19]T. R. Kukreja, D. Kumar, K. Prasad, R. C. Chauhan, S. Choe, and P. P. Kundu, *Eur. Polym. J.* **38**, 1417 (2002).

[20]R. Rajan, S. Varghese, M. Balachandran, and K. E. George, RUBBER CHEM. TECHNOL. **89**, 211 (2016).

[21]L. Li, Y.-J. Choi, K. Boonkerd, J. Zhang, L. J. Gao, Z. X. Zhang, and J. K. Kim, RUBBER CHEM. TECHNOL. **86**, 190 (2013).

[22]G. Allegra, G. Raos, and M. Vacatello, *Prog. Polym. Sci.* **33**, 683 (2008).

[23]C. S. Barrera and K. Cornish, *J. Polym. Environ.* **23**, 437 (2015).

[24]A. Voelkel, B. Strzemiecka, K. Adamska, and K. Milczewska, *J. Chromatogr. A* **1216**, 1551 (2009).

[25]M. Rückriem, A. Inayat, D. Enke, R. Gläser, W.-D. Einicke, and R. Rockmann, *Colloids Surfaces A Physicochem. Eng. Asp.* **357**, 21 (2010).

[26]M. N. Belgacem, G. Czeremuszkin, S. Sapieha, and A. Gandini, *Cellulose* **2**, 145 (1995).

[27]S. C. Das, I. Larson, D. A. V. Morton, and P. J. Stewart, *Langmuir* **27**, 521 (2011).

[28]B. Charmas and R. Leboda, *J. Chromatogr. A* **886**, 133 (2000).

[29]F. Thielmann, *J. Chromatogr. A* **1037**, 115 (2004).

[30]S. Brunauer, P. H. Emmett, and E. Teller, *J. Am. Chem. Soc.* **60**, 309 (1938).

[31]E. P. Barrett, L. G. Joyner, and P. P. Halenda, *J. Am. Chem. Soc.* **73**, 373 (1951).

[32]C. S. Barrera and K. Cornish, *Ind. Crops Prod.* **86**, 132 (2016).

[33]S. S. Shapiro and M. B. Wilk, *Biometrika* **52**, 591 (1965).

[34]I. T. Jolliffe, *Principal Component Analysis*, vol. 30, Springer-Verlag, New York, 2002.

[35]S. A. Abdul-Wahab, C. S. Bakheit, and S. M. Al-Alawi, *Environ. Model. Software* **20**, 1263 (2005).

[36]H. Çamdevýren, N. Demýr, A. Kanik, and S. Keskýn, *Ecol. Modell.* **181**, 581 (2005).

[37]A. K. Plappally, I. Yakub, L. C. Brown, W. O. Soboyejo, and A. B. O. Soboyejo, *J. Eng. Mater. Technol.* **133**, 31004 (2011).

[38]A. B. Soboyejo, *Probabilistic Methods in Engineering and Biosystems Engineering*, 2011.

[39]R Core Team, R Foundation for Statistical Computing, Vienna, Austria, 2014.

[40]E. Papirer, E. Brendle, F. Ozil, and H. Balard, *Carbon N. Y.* **37**, 1265 (1999).

[41]E. Papirer, H. Balard, and A. Vidal, *Eur. Polym. J.* **24**, 783 (1988).

[42]M. Gerspacher and W. Wampler, in *Basic Elastomer Technology*, K. C. Baranwal and H. Stephens, Eds., American Chemical Society, Rubber Division, Akron, OH, 2001, pp. 57–81.

[43]N. Sombatsompop, S. Thongsang, T. Markpin, and E. Wimolmala, *J. Appl. Polym. Sci.* **93**, 2119 (2004).

[44]B. G. Kutchko and A. G. Kim, *Fuel* **85**, 2537 (2006).

[45]P. E. Kolattukudy, *Science* **208**, 990 (1980).

[46]Y. Wang, X. Li, G. Sun, D. Li, and Z. Pan, *J. Food Eng.* **126**, 27 (2014).

[47]A.-L. Fameau, C. Gaillard, D. Marion, and B. Bakan, *Green Chem.* **15**, 341 (2013).

[48]D. Rasutis, K. Soratana, C. Mcmahan, and A. E. Landis, *Ind. Crop. Prod.* **70**, 383 (2015).

[49]F. S. Nakayama, *Ind. Crops Prod.* **22**, 3 (2005).

[50]P. S. Guru and S. Dash, *Adv. Colloid Interface Sci*. **209**, 49 (2014).

[51]P. Intharapat, A. Kongnoo, and K. Kateungngan, *J. Polym. Environ*. **21**, 245 (2013).

[52]W. M. Burry and D. S. Keller, *J. Chromatogr. A* **972**, 241 (2002).

[53]W. T. Tsai, J. M. Yang, C. W. Lai, Y. H. Cheng, C. C. Lin, and C. W. Yeh, *Bioresour. Technol*. **97**, 488 (2006).

[54]S. Bandyopadhyay-Ghosh, S. B. Ghosh, and M. Sain, in *Biofiber Reinforcements in Composite Materials*, O. Faruk and M. Sain, Eds., Elsevier, Sawston, Cambridge, 2015.

[55]W. W. Schloman, *Ind. Crops Prod.* **22**, 41 (2005).

[56]L. F. Ramos-de Valle, *J. Rheol. (N. Y. N. Y)*. **25**, 379 (1981).

[*Received October 2016, Revised January 2017*]